Trapped topoisomerase II initiates formation of de novo duplications via the nonhomologous end-joining pathway in yeast

Nicole Stantial[a,1], Anna Rogojina[b,1,2], Matthew Gilbertson[b,3], Yilun Sun[b,4], Hannah Miles[b,5], Samantha Shaltz[a], James Berger[c], Karin C. Nitiss[b], Sue Jinks-Robertson[a,6], and John L. Nitiss[b,6]

[a]Department of Molecular Genetics and Microbiology, Duke University Medical Center, Durham, NC 27710; [b]Pharmaceutical Sciences Department, University of Illinois at Chicago, Rockford, IL 61107; and [c]Department of Biophysics and Biophysical Chemistry, Johns Hopkins School of Medicine, Baltimore, MD 20215

Contributed by Sue Jinks-Robertson, August 28, 2020 (sent for review May 4, 2020; reviewed by Rodney Rothstein and Thomas E. Wilson)

Topoisomerase II (Top2) is an essential enzyme that resolves catenanes between sister chromatids as well as supercoils associated with the over- or under-winding of duplex DNA. Top2 alters DNA topology by making a double-strand break (DSB) in DNA and passing an intact duplex through the break. Each component monomer of the Top2 homodimer nicks one of the DNA strands and forms a covalent phosphotyrosyl bond with the 5′ end. Stabilization of this intermediate by chemotherapeutic drugs such as etoposide leads to persistent and potentially toxic DSBs. We describe the isolation of a yeast *top2* mutant (*top2-F1025Y,R1128G*) the product of which generates a stabilized cleavage intermediate in vitro. In yeast cells, overexpression of the *top2-F1025Y,R1128G* allele is associated with a mutation signature that is characterized by de novo duplications of DNA sequence that depend on the nonhomologous end-joining pathway of DSB repair. Top2-associated duplications are promoted by the clean removal of the enzyme from DNA ends and are suppressed when the protein is removed as part of an oligonucleotide. *TOP2* cells treated with etoposide exhibit the same mutation signature, as do cells that overexpress the wild-type protein. These results have implications for genome evolution and are relevant to the clinical use of chemotherapeutic drugs that target Top2.

Top2 | yeast | mutagenesis | etoposide | nonhomologous end joining

Topoisomerases are enzymes that transiently cut DNA in a highly regulated fashion to carry out topological alterations. Type I topoisomerases are typically monomers that make single-strand breaks in DNA while type II enzymes are homodimers that cleave both DNA strands to create double-strand breaks (DSBs) (1–3). The ability to cut DNA is absolutely required to change DNA topology and cleavage occurs through formation of a transient, covalent phosphotyrosyl linkage with DNA. Type IA and IB enzymes create 5′- and 3′-phosphotyrosyl links, respectively, while type II enzymes form a 5′-phosphotyrosyl link. The resulting single- or double-strand break alters DNA winding using a swiveling (type IB) or strand passage mechanism (type IA and type II), after which the phosphotyrosyl bond is reversed to restore the phosphodiester backbone of the DNA. While the use of a covalent enzyme-DNA intermediate makes cleavage and rejoining a relatively error-free process, any DNA breakage is potentially dangerous (4). If DNA is cut and the break persists, a DNA damage response is activated that leads to cell-cycle arrest, senescence, or apoptosis (5–7). Stabilization of covalent DNA-topoisomerase intermediates has been exploited to identify and develop therapeutic small molecules such as fluoroquinolone antibiotics and a variety of anticancer drugs (8, 9). These inhibitory molecules have also been very useful as probes for enzyme mechanism (10–12).

In addition to small molecules that trap topoisomerases on DNA, a variety of DNA structural alterations can affect cleavage and religation. For type I enzymes, DNA lesions that include abasic sites, nicks, base-base mismatches, and base alterations can lead to enhanced DNA cleavage in vitro and in vivo (13–15). Notably, single ribonucleotides embedded in duplex DNA lead to elevated cleavage by type IB topoisomerases in vitro (16) and are associated with a distinctive mutation signature in vivo (17). In the yeast *Saccharomyces cerevisiae*, this signature is composed of deletions that remove a single unit from a tandem repeat and reflects sequential cleavage of the same DNA strand by topoisomerase I (Top1) (18–20). Type II topoisomerases can also be trapped on DNA by structural alterations, although the range of lesions appears more limited than for type I enzymes (21). Lesions that can trap eukaryotic type II topoisomerases include abasic sites (22) and mis-incorporated ribonucleotides (23).

Significance

Transcription and replication of DNA create topological problems that are resolved by topoisomerases. These enzymes nick DNA strands to allow strand passage and then reseal the broken DNA to restore its integrity. Topoisomerase II (Top2) nicks complementary DNA strands to create double-strand break (DSB) intermediates that can be stabilized by chemotherapeutic drugs and are toxic if not repaired. We identified a mutant form of yeast Top2 that forms stabilized cleavage intermediates in the absence of drugs. Overexpression of the mutant Top2 was associated with a unique mutation signature in which small, unique segments of DNA are duplicated. These de novo duplications required the nonhomologous end-joining pathway of DSB repair, and their Top2 dependence has clinical and evolutionary implications.

Author contributions: N.S., K.C.N., S.J.-R., and J.L.N. designed research; N.S., A.R., M.G., Y.S., H.M., S.S., and K.C.N. performed research; N.S., A.R., M.G., Y.S., H.M., S.S., J.B., S.J.-R., and J.L.N. analyzed data; and N.S., J.B., S.J.-R., and J.L.N. wrote the paper.

Reviewers: R.R., Columbia University Medical Center; and T.E.W., University of Michigan Medical School.

The authors declare no competing interest.

[1]N.S. and A.R. contributed equally to this work.

[2]Present address: Greehey Children's Cancer Research Institute, University of Texas Health Science Center, San Antonio, TX 78229.

[3]Present address: Department of Gene and Cell Therapies, PPD, Inc., Middleton, WI 53562.

[4]Present address: Laboratory of Molecular Pharmacology and Developmental Therapeutics Branch, Center for Cancer Research, National Cancer Institute, National Institutes of Health, Bethesda, MD 20892.

[5]Present address: Department of Pharmaceutical Sciences, University of Wisconsin, Madison, WI 53705.

[6]To whom correspondence may be addressed. Email: sue.robertson@duke.edu or jlnitiss@uic.edu.

This article contains supporting information online at https://www.pnas.org/lookup/suppl/doi:10.1073/pnas.2008721117/-/DCSupplemental.

First published October 12, 2020.

The trapping of both subunits of Top2 results in a DSB, while the trapping of only a single subunit leads to a persistent single-strand nick.

The study of cytotoxic and mutagenic mechanisms of elevated topoisomerase cleavage has been facilitated by the identification of mutants that are proficient for DNA cleavage but defective in religation (24–26). While mutations that result in stabilized cleavage intermediates have been readily obtained in yeast *TOP1*, few examples have been identified for type II topoisomerases. The sole exception is a mutant form of human TOP2α (Asp48 changed to Asn) identified in a screen for mutations affecting the action of bisdioxopiperazines (27). Similar to yeast *top1* mutants, the human TOP2α^{D48N} mutant exhibits elevated DNA cleavage in vitro and cannot be expressed in recombination-defective (*rad52*Δ) yeast cells. We describe here a mutant yeast Top2 protein (Top2-F1025Y,R1128G; abbreviated Top2-FY,RG) that similarly is lethal when overexpressed in a *TOP2 rad52*Δ background and leads to elevated DNA cleavage in vitro. The corresponding amino acid changes, however, are in the C-terminal dimerization domain of Top2, thereby implicating this domain in the regulation of DNA cleavage and/or religation by the enzyme. Top2-FY,RG overexpression elevates homologous recombination and spontaneous mutagenesis and is associated with a distinctive mutation signature (de novo duplications) that is dependent on the nonhomologous end-joining (NHEJ) pathway of DSB repair. Similar de novo duplications were observed following treatment of wild-type (WT) cells with etoposide, a chemotherapeutic drug that stabilizes the covalent Top2 cleavage intermediate. Finally, we implicate WT Top2 as the source of rare de novo duplications observed previously in frameshift reversion assays (28). These data suggest important roles for Top2-dependent mutagenesis in genome evolution as well as in genetic stability following chemotherapy.

Results

C-Terminal *TOP2* Mutations Confer Hypersensitivity to Etoposide. We previously described mutations in yeast *TOP2* that result in hypersensitivity to different classes of Top2-targeting agents such as etoposide and mAMSA (29). To identify additional mutations conferring this phenotype, we carried out a screen following the introduction of random mutations by error-prone PCR into a DNA segment specifying amino acids 900 to 1,250. The mutagenized fragment was recombined into gapped plasmid pDED1Top2 (29, 30) by cotransformation of the gapped plasmid and the mutagenized fragment into a temperature-sensitive *top2-4* strain (31). Expression of *TOP2* in strains carrying pDED1Top2 results in ∼10-fold more protein than does expression from the native *TOP2* promoter (30). Transformants were selected at 34 °C, which is nonpermissive for the *top2-4* allele, to limit the isolation of plasmids carrying *top2* null alleles. Individual colonies were screened for sensitivity to mAMSA on solid medium, and two mutants with alterations in the C-terminal part of the cleavage/ligation domain of Top2 were identified. The first mutant had Arg1128 changed to Gly (R1128G) while the second (independent) mutant had the R1128G change plus an additional mutation that converted Phe1025 to Tyr (F1025Y).

The F1025Y and R1128G changes (FY and RG, respectively) were reintroduced into the pDED1Top2 plasmid individually or together by site-directed mutagenesis. Following introduction into the *top2-4* background, transformants were assessed for survival following exposure to varying concentrations of mAMSA or etoposide at 34 °C. *top2-4* cells carrying the pDED1Top2 or pDED1Top2-FY plasmid were insensitive to mAMSA even at a concentration of 50 μg/mL (*SI Appendix*, Fig. S2*A*). By contrast, cells containing the *top2-RG* or *top2-FY,RG* allele were sensitive to 5 μg/mL mAMSA. *top2-4* cells carrying the pDED1Top2 plasmid were modestly sensitive to etoposide (Fig. 1*A*) and those with the pDED1Top2-RG plasmid were more sensitive to the drug. Although overexpressing the *top2-FY* allele alone did not enhance etoposide sensitivity relative to the *TOP2* control, the double-mutant *top2-FY,RG* allele was associated with a high level of drug sensitivity. Based on drug-sensitivity profiles, only strains containing the plasmid-encoded *top2-RG* or *top2-FY,RG* allele were further analyzed.

Expression of *top2-RG* or *top2-FY,RG* Is Lethal in the Absence of *RAD52*. Previous drug-hypersensitive *top2* mutants were viable in a *rad52*Δ background that is unable to repair DSBs (34). We were unable, however, to obtain colonies at 34 °C following the transformation of either the pDED1Top2-RG or pDED1Top2-FY,RG plasmid into a *top2-4 rad52*Δ strain. To more rigorously demonstrate lethality of the *top2* alleles in the absence of recombination, we introduced a plasmid containing a *pGAL-RAD52* fusion into a *top2-4 rad52*Δ background. Cells were thus phenotypically

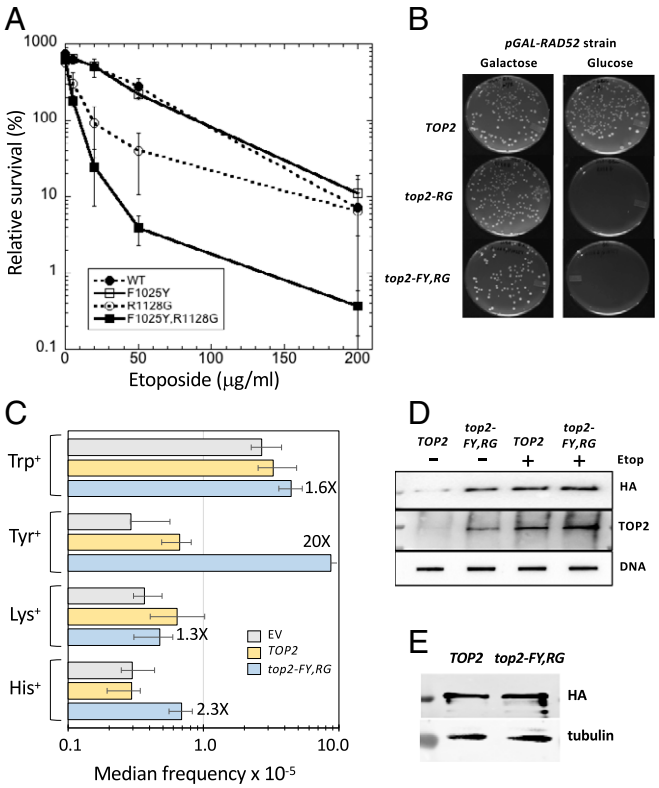

Fig. 1. Genetic characterization of *top2* mutants. (*A*) The *top2-4* host strain, JN362at2-4 (30), was transformed with pDED1Top2 plasmids containing the indicated alleles. Transformants were grown to midlog phase in SC-Ura medium at 34 °C, and the indicated concentration of etoposide was added. Incubation was continued for an additional 24 h before plating cells for survival. The survival plotted is relative to that at the time of etoposide addition. Error bars are ± SEM. (*B*) The pGAL-Rad52 plasmid (32) was transformed into a *top2-4 rad52*Δ background (JN332at2-4), and then cells grown in galactose medium were transformed with pDED1Top2 containing the indicated allele. Transformants were selected on uracil-deficient medium containing either glucose or galactose as a carbon source. (*C*) Diploid strain CG2009 was transformed with the relevant plasmid and grown selectively in SC/peptone-Ura medium prior to plating on drop-out media (SC/peptone) to select recombinants. Error bars are 95% confidence intervals. (*D*) YMM10t2-4, a *top2-4* derivative of YMM10 (33), was transformed with the pDED1Top2 or pDED1Top2-FY,RG plasmid containing an HA-tagged allele. Transformants were grown in the presence or absence of 200 μg/mL etoposide prior to genomic DNA isolation using the yeast ICE protocol. After DNA recovery, quantitation, and digestion with micrococcal nuclease, DNA-associated proteins were separated by SDS/PAGE, and Top2 was detected using an anti-HA or anti-TOP2 antibody. Survival data following 24 h growth in the presence of mAMSA are shown in *SI Appendix*, Fig. S2. (*E*) Top2 and Top2-FY,RG levels relative to tubulin are shown.

Rad52$^+$ or Rad52$^-$ on galactose- or glucose-containing medium, respectively. Cells transformed with pDED1Top2 grew well on both types of plates, while those carrying the mutant pDED1Top2-RG or pDED1Top2-FY, RG plasmid formed colonies only on galactose-containing medium (Fig. 1*B*). This effect was verified by streaking colonies obtained on galactose medium in parallel onto medium containing either glucose or galactose.

Given the requirement for homologous recombination functions for survival, we hypothesized that expression of the mutant Top2 proteins would confer a hyper-recombination phenotype. The double-mutant plasmid, WT pDED1Top2, or the empty vector (EV) YCp50 (35) thus was introduced into a diploid yeast strain carrying multiple heteroallelic markers. Recombination frequencies were measured by selecting for tryptophan, lysine, histidine, or tyrosine prototrophs. Relative to the EV control, overexpression of *TOP2* from *pDED1* did not enhance recombination frequencies between any of the heteroallelic pairs examined (Fig. 1*C*). Overexpression of the *top2-FY,RG* allele, however, resulted in 2.3-fold increase in His$^+$ recombinants and a 20-fold increase in Tyr$^+$ recombinants; there was no significant increase in Lys$^+$ or Trp$^+$ recombinants. The reason for the variable recombination effects of the *top2-FY,RG* allele is unclear, but could reflect the relative distances between heteroalleles at the loci monitored, differing levels of gene expression, preferred sites of Top2 cleavage, or other features related to local chromosome structure.

Top2-FY,RG Is Trapped on Yeast DNA in the Absence of Etoposide. Top2 poisons such as etoposide interfere with DNA religation catalyzed by the enzyme and create DNA damage in the form of strand breaks with covalently attached protein at the ends. Adducts formed in vivo can be detected using an in vivo complex of enzyme (ICE) assay that immunologically detects protein covalently associated with DNA (33, 36). For the ICE assay in yeast, we constructed variants of WT and double-mutant pDED1 plasmids in which the C terminus of the Top2 protein was tagged with hemagglutinin (HA). These variants were then expressed in a *top2-4* strain with increased etoposide sensitivity due to the absence of multiple drug-efflux pumps (33). Cells expressing WT *TOP2* showed a faint Top2 signal that was greatly enhanced when cells were treated with etoposide (Fig. 1*D*). By contrast, cells expressing the double-mutant allele showed a robust signal in the absence of etoposide that was further enhanced by drug treatment. Given the similar levels of the Top2 and Top2-FY,RG proteins (Fig. 1*E*), we conclude that Top2-FY,RG is a self-poisoning enzyme that frequently becomes trapped on DNA in the absence of etoposide.

Relaxation and Cleavage Activities of Mutant Top2 Proteins. For biochemical characterization of Top2-RG and Top2-FY,RG, the relevant mutations were introduced into plasmid pGAL1Top2 (37). The proteins were then overexpressed in and purified from a *top1*Δ background in order to eliminate the confounding effects of Top1 activity. The relaxation activities of the purified proteins were assessed using negatively supercoiled pUC18 DNA as substrate (38). Under our standard conditions, complete relaxation of pUC18 by the WT or Top2 mutant proteins required 25 to 50 ng of protein (Fig. 2*A*). This result indicates that the overall catalytic activity of the mutant proteins was similar to that of WT yeast Top2. We next examined the ability of the mutant Top2 proteins to cleave pUC18 DNA in the absence of Top2-targeting agents. Double-strand DNA cleavage of plasmid DNA results in the formation of linear DNA molecules. For WT Top2, a very faint linear band was seen with 150 ng of purified protein (Fig. 2*B*). By contrast, linear fragments were observed with Top2-RG and Top2-FY,RG at protein concentrations as low as 50 ng. We also examined the response of Top2-RG and Top2-FY,RG to etoposide (Fig. 2*C*) and mAMSA (*SI Appendix*, Fig. S2*B*). In the presence of these small-molecule inhibitors, the mutant proteins were associated with a higher level of linear DNA as the drug concentration was increased. At higher etoposide concentrations (e.g., Top2-RG at etoposide concentrations greater than 1 μg/mL), smearing of DNA was observed, which presumably represents plasmids cleaved at two or more separate sites. These results demonstrate that the purified Top2-RG and Top2-FY,RG proteins have an intrinsic hypersensitivity to mAMSA and etoposide that is in agreement with the phenotypes of Top2-RG and Top2-FY,RG in vivo.

The catalytic cycle of Top2 is illustrated in Fig. 3*A*. Although ATP is required for supercoil relaxation and for decatenation by Top2, eukaryotic Top2 cleaves DNA, albeit at a much lower level, even in the absence of ATP (3). We were interested in determining whether the mutants that resulted in elevated DNA cleavage required progression through the catalytic cycle and were specifically defective in religation after strand passage had occurred. To test this possibility, we examined stable cleavage of pUC18 DNA by the WT and mutant proteins in the absence of ATP (Fig. 3*B*). For WT Top2, linearization of pUC18 was barely detectable, although DNA nicking was seen. By contrast, linearized DNA was readily detected when pUC18 was incubated with 1 μg Top2-RG or 0.3 μg Top2-FY,RG. These results demonstrate that ATP is not required for elevated DNA cleavage by the mutant proteins, although it still strongly potentiates cleavage. Because ATP (or a nonhydrolyzable analog) is required for progression through the catalytic cycle and for strand passage, these results suggest that progression of the catalytic cycle is not required for elevated, drug-independent cleavage of DNA by these proteins.

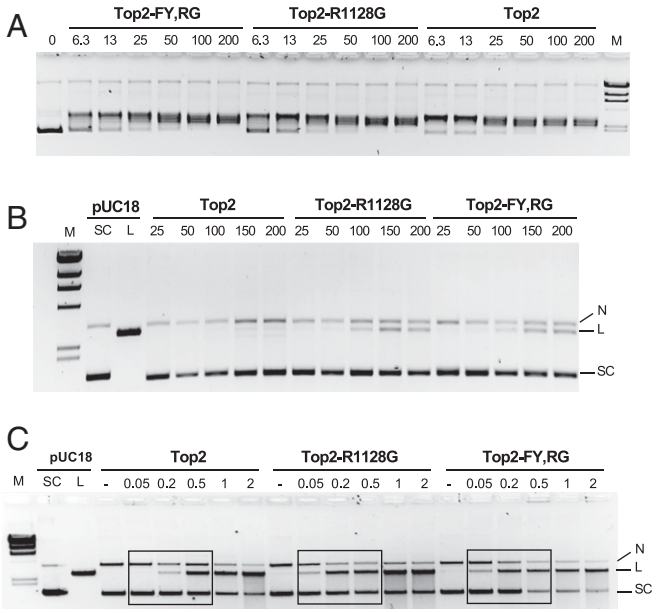

Fig. 2. Biochemical activities of WT and mutant proteins. Top2 proteins were expressed from the *pGAL1* promoter in the *top1*Δ strain JELt1 (29), and 200 ng of negatively supercoiled pUC18 DNA was used in all reactions. (*A*) DNA strand-passage activity of purified WT, Top2-R1128G, and Top2-FY,RG proteins; the amount of protein (ng) is indicated above each lane. (*B*) DNA cleavage activity of WT and mutant Top2 proteins; the positions of nicked (N), linear (L), and supercoiled (SC) pUC18 are indicated. DNA cleavage is quantitated in *SI Appendix*, Fig. S1. (*C*) DNA cleavage activity of WT and mutant Top2 proteins in the presence of etoposide; etoposide concentration (μg/mL) is indicated above each lane. Data in the presence of mAMSA are in *SI Appendix*, Fig. S2.

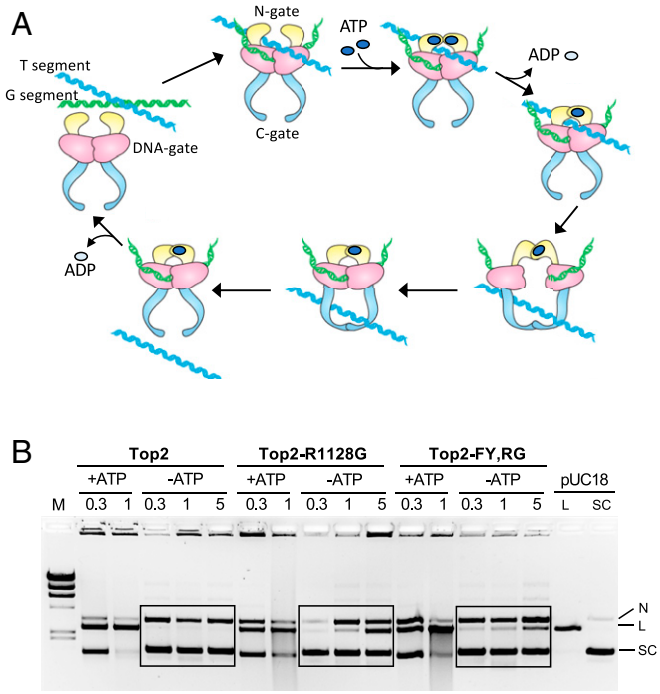

Fig. 3. Progression through the Top2 catalytic cycle is not required for elevated cleavage. (*A*) The catalytic cycle of eukaryotic Top2 is illustrated (2). Top2 cleaves DNA in the presence of a divalent cation but cannot proceed to strand passage without ATP binding (blue circles) and dimerization of the N-gate (yellow). The two ATP molecules are hydrolyzed sequentially. Strand passage through the G segment (green) is followed by religation and release of the T segment (blue) through the C-gate. (*B*) DNA cleavage activity of purified WT and mutant Top2 proteins in the presence or absence of ATP; protein concentration (μg) is indicated above each lane. Positions of nicked (N), linear (L), and supercoiled (SC) pUC18 are indicated.

Top2-FY,RG Is Mutagenic and Is Associated with de Novo Duplications. Expression of the *top2-FY,RG* allele resulted in a hyper-recombination phenotype and was lethal in a *rad52*Δ background (Fig. 1), consistent with formation of potentially toxic DSBs. In vitro, the mutant protein generated persistent nicks as well as DSBs (Fig. 2), leading us to examine whether its expression might be mutagenic. For this analysis, the EV, pDEDTop2, or pDED1Top2-FY,RG plasmid was introduced into a haploid *TOP2* background. The *CAN1* forward-mutation assay was used to measure mutation rates and analyze mutation types. In this assay, any mutation that disables the function of the encoded protein confers resistance to canavanine, a toxic arginine analog. The canavanine-resistance (Can-R) rate was indistinguishable in cells containing either the EV or pDED1Top2. By contrast, expression of the *top2-FY,RG* allele elevated the Can-R rate 2.7-fold (*SI Appendix*, Table S1).

Approximately 75% of *can1* mutations detected were base substitutions when either the EV or the pDED1Top2 plasmid was present (105/142 and 111/155, respectively; $P = 0.74$ by contingency χ^2; see *SI Appendix*, Table S2, for complete spectra). By contrast, only 28% of mutations were base substitutions in the strain containing the pDED1Top2-FY,RG plasmid (50/176; $P < 0.0001$). The proportional decrease in base substitutions was accompanied by a large increase in insertions of more than one base pair (1 bp; from 2/142 with the EV to 75/176; $P < 0.0001$). Most of these insertions (49/75) corresponded to de novo duplications, which are defined as the creation of a repeat where one did not previously exist. In the segment of the *CAN1* open reading frame shown in Fig. 4*A*, for example, CTGT (nucleotide [nt] 1,239 to 1,242) became CTGTCTGT in one mutant, and CATT (nt 1,272 to 1,275) was duplicated to CATTCATT in another. The remainder of insertions >1 bp occurred within a preexisting repeat; because of the genetic requirements for their formation (see below), we consider these jointly with the de novo duplications. The most frequent size of duplications was 4 bp (*SI Appendix*, Table S2), which matches the distance between Top2-generated nicks in vitro (39) and is relevant to the proposed mechanism of duplication formation (*Discussion*).

The rates of specific mutation types (base substitutions, 1-bp deletions, 1-bp insertions, de novo duplications, and others) in the presence of the EV, the pDED1Top2, or the pDED1Top2-FY,RG plasmid are presented in Fig. 4*B*. We estimate an ∼80-fold increase in the rate of duplications, but no change in the base substitution rate, when the *top2-FY,RG* allele was overexpressed. It should be noted that there was also a 7.6-fold increase in the rate of +1 insertions associated with pDED1Top2-FY,RG. Although most of these 1-bp insertions were in short homopolymer runs and could reflect DNA polymerase slippage during replication, their increase suggests that many were likely generated by the same mechanism as the larger insertions.

Top2 Overexpression Elevates Duplications in Frameshift Reversion Assays. Although there was no increase in the overall rate of Can-R in the presence of the pDED1Top2 plasmid, there was an

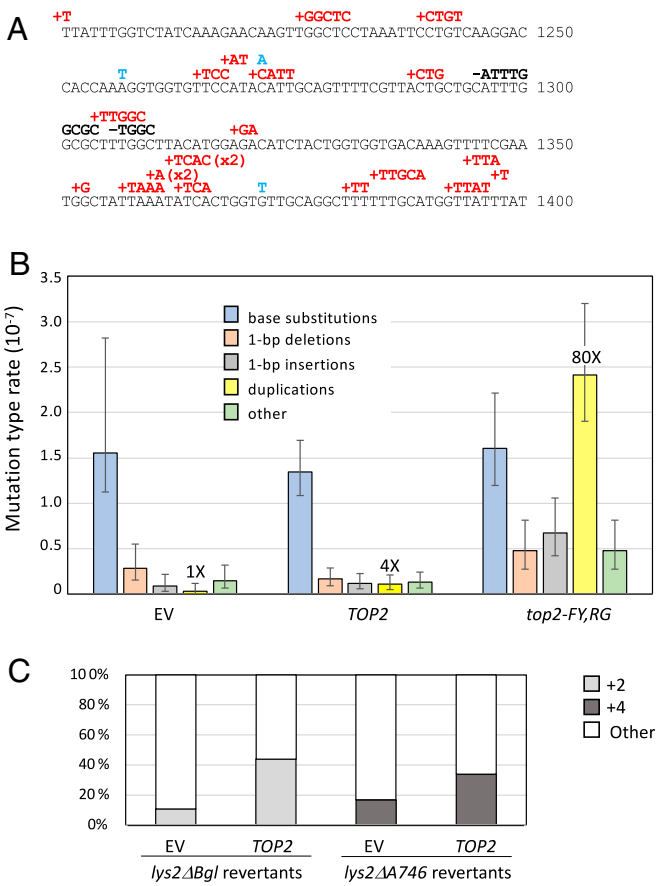

Fig. 4. Top2-FY,RG expression is associated with de novo duplications. (*A*) Partial *CAN1* mutation spectrum. Mutations are above the sequence; insertions are in red font, base substitutions in blue font, and deletions in black font. (*B*) Rates of specific mutation types in a *TOP2* strain containing the EV, pDED1Top2, or pDED1Top2-FY,RG. Error bars are 95% confidence intervals. (*C*) Proportions of 2- and 4-bp duplications among Lys$^+$ revertants of the *lys2ΔBgl,NR* (SJR1467) and *lys2ΔA746,NR* (SJR1468) alleles (28). Can-R rates and associated spectra are in *SI Appendix*, Tables S1 and S2. Complete Lys$^+$ spectra are in *SI Appendix*, Fig. S3.

approximately four-fold increase in duplications. Given their small number, however, neither the proportional increase in these events (2/142 for EV and 9/155 for pDED1Top2; $P = 0.09$) nor their corresponding rate significantly increased relative to cells that did not overexpress Top2. To focus specifically on 2- and 4-bp duplications, we used frameshift-reversion assays where similar events were previously observed (28). The *lys2ΔBgl,NR* allele reverts by acquisition of a net −1 frameshift and so can detect 2-bp insertions; the *lys2ΔA746,NR* reverts by net +1 frameshifts, which includes 4-bp insertions. Top2 overexpression was accompanied by a proportional increase in 2-bp (from 3/28 to 22/50; $P = 0.0056$) and 4-bp duplications (from 6/36 to 33/98, $P = 0.088$; Fig. 4*C* and *SI Appendix*, Fig. S3). When these events were jointly considered, their increase was highly significant ($P = 0.0014$), demonstrating an association of a specific class of mutations with Top2 overexpression.

Top2cc-Dependent Duplications Require the NHEJ Pathway. In vitro, the Top2-FY,RG protein generates nicks in addition to DSBs (Fig. 2), either of which potentially could initiate the de novo sequence duplications observed in vivo. Because the NHEJ pathway can introduce sequence changes at the junction of joined ends and was previously implicated in generating the de novo duplications in the frameshift-reversion assays described above (28), we examined the relevance of this pathway to the mutagenesis associated with stabilization of the Top2 cleavage complex (Top2cc; Fig. 5*A* and *SI Appendix*, Tables S1 and S2). We first deleted the *DNL4* gene, which encodes the DNA ligase required for NHEJ (40) in cells containing the pDED1Top2-FY,RG plasmid. In the *dnl4*Δ background, there was a 40% reduction in the Can-R rate that was accompanied by a large proportional decrease in de novo duplications (from 75/176 to 7/194; $P < 0.0001$) as well as 1-bp insertions (from 21/176 to 7/194; $P = 0.005$). The Ku complex is also required for NHEJ in yeast, and results in the *ku70*Δ background were similar to those obtained in the *dnl4*Δ background (*SI Appendix*, Table S1). In addition to the requirement for Dnl4 and Ku, most end-/gap-filling that occurs during NHEJ requires DNA polymerase 4 (Pol4). Deletion of *POL4* from the strain containing the pDED1Top2-FY,RG plasmid also significantly reduced the Can-R rate and the proportion of duplications (from 75/176 to 25/126; $P < 0.0001$). The effect of *POL4* loss on duplications, however, was not as dramatic as that observed in the absence of *DNL4* (25/126 and 7/194, respectively; $P < 0.0001$). Loss of *POL4* had no effect on 1-bp insertions (21/176 and 12/126 in WT and *pol4*Δ, respectively; $P = 0.63$), which is consistent with its reduced requirement for duplications and the relatively high background of +1 events. Together, these data demonstrate that the majority of sequence duplications in this system are products of Top2-generated DSBs that are repaired by NHEJ.

Pathways for Top2cc Removal Affect Duplication Rates. A stabilized yeast Top2cc can potentially be removed by either 1) proteolytic degradation followed by peptide extraction through cleavage of the phosphotyrosyl bond or 2) nuclease-dependent removal of a Top2-linked oligonucleotide. In the first pathway, the Top2 peptide that remains after proteolysis is removed by tyrosyl-DNA phosphodiesterase 1 (Tdp1) (41). Although *TDP1* loss had no significant effect on the Can-R rate in the presence of the pDED1Top2-FY,RG plasmid, there was a large proportional reduction in duplications (75/176 to 11/205; $P < 0.0001$) and 1-bp insertions (21/176 to 7/205; $P = 0.003$), and rates of these events were significantly reduced (Fig. 5*B* and *SI Appendix*, Tables S1 and S2).

In higher eukaryotes, a major pathway for Top2cc removal from a DNA end is by the endonuclease activity of the MRE11 component of the MRN (MRE11-RAD50-NBS1) complex, which releases a Top2-linked oligonucleotide (42). In *S. cerevisiae*, Mre11-Rad50-Xrs2 (MRX) is the equivalent complex,

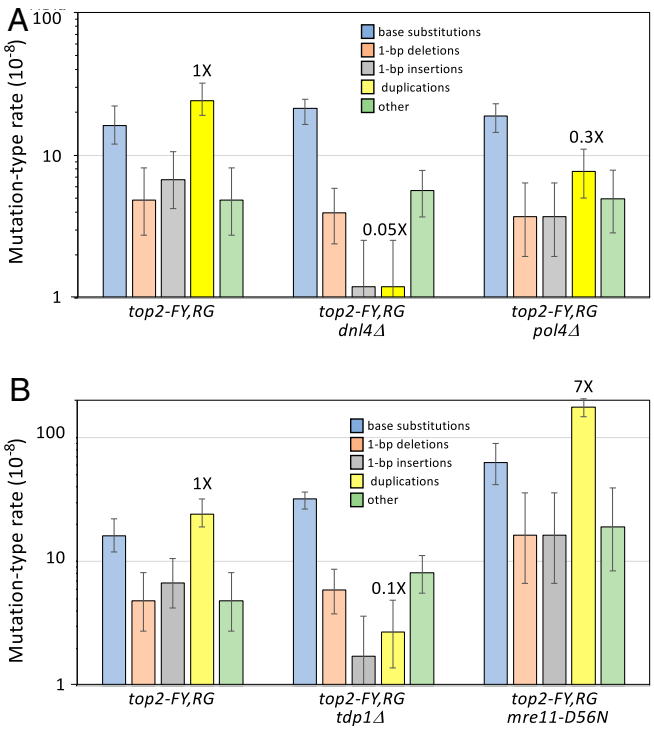

Fig. 5. Genetic control of mutations associated with *top2-FY,RG* expression. Indicated candidate genes were deleted in the *TOP2* background, and the resulting strains were transformed with EV, pDED1Top2, or pDED1Top2-FY,RG. (*A*) Duplications require Dnl4 and partially require Pol4. (*B*) Duplications are promoted by Tdp1 and suppressed by the nuclease activity of Mre11 (*mre11-D56N*). Rates and associated spectra are in *SI Appendix*, Tables S1 and S2. The fold change in duplication rate in each mutant relative to the WT background (1.0×) is indicated.

and loss of any of the component proteins confers etoposide hypersensitivity (43). Although we were unable to obtain colonies following transformation of *mre11*Δ cells with the pDED1Top2-FY,RG plasmid, transformants were readily obtained in a background containing the nuclease-dead *mre11-D56N* allele (44). The essential role of yeast MRX in dealing with Top2-associated damage is thus distinct from its nuclease activity. Expression of the *top2-FY,RG* allele in an *mre11-D56N* background was associated with a 7.3-fold increase in the rate of de novo duplications (Fig. 5*B*), indicating that Mre11 nuclease activity is primarily responsible for yeast Top2cc removal from DNA ends. In its absence, the phosphotyrosyl peptide that remains after Top2 proteolysis is cleanly removed by Tdp1, and the ends give rise to NHEJ-dependent duplications.

Mutagenic Effects of Etoposide. To further examine the dependence of duplications on Top2cc stabilization, we isolated Can-R mutants in a drug-sensitized *TOP2* strain grown in the presence of either dimethylsulfoxide (DMSO), the vehicle for etoposide, or DMSO plus 200 μg/mL etoposide. Although etoposide did not alter the median Can-R frequency (*SI Appendix*, Table S3), there were significant changes in the corresponding spectrum and in the frequencies of some mutation types (Fig. 6 and *SI Appendix*, Table S3). Relative to the DMSO-treated cultures, there was a proportional increase in duplications (from 1/162 to 36/222; $P < 0.0001$) as well as 1-bp insertions (from 3/162 to 19/222; $P < 0.0001$) in the presence of etoposide. Confirmation that the mutagenic effect of etoposide was mediated through Top2cc stabilization was obtained using the etoposide resistant *top2-5* allele (45). Because this allele confers temperature sensitivity, experiments were performed at room temperature (RT) rather than at

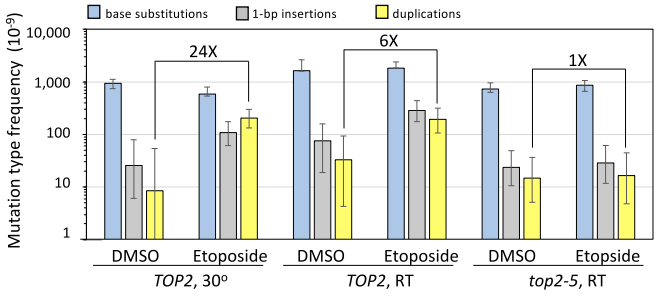

Fig. 6. Etoposide stimulates duplications through its interaction with Top2. A *TOP2 pdr1DBD-CYC8::LEU2* (drug-sensitized) strain was grown in the presence of DMSO or DMSO+etoposide at RT or at 30 °C. The temperature-sensitive *top2-5 pdr1DBD-CYC8::LEU2* strain only grows at RT and is etoposide resistant. Median Can-R frequencies were determined rather than rates because of the variation in the number of viable cells in etoposide-treated cultures; error bars are 95% confidence intervals. Median frequencies and associated spectra are in *SI Appendix*, Tables S2 and S3.

30 °C. Interestingly, the Can-R frequency in the WT strain was elevated approximately two-fold when cells were grown at RT in the presence of DMSO or etoposide (Fig. 6 and *SI Appendix*, Table S3). As at 30 °C, however, etoposide treatment of the WT strain at RT stimulated duplications (from 4/288 to 18/305; $P = 0.007$) and 1-bp insertions (9/288 and 27/305; $P = 0.006$), and their rates were not significantly different from those observed at 30 °C. By contrast, etoposide stimulated neither duplications (5/344 in DMSO and 4/297 in etoposide, respectively; $P = 1$) nor 1-bp insertions (8/344 and 7/297; $P = 1$) in the *top2-5* background.

Discussion

Topoisomerases carry out essential reactions that require DNA cleavage and a failure to quickly religate DNA can lead to genome destabilization (21). In the current study, we identified and characterized yeast *top2* alleles (*top2-R1128G* and *top2-F1025Y,R1128G*) that produce proteins that are defective in quickly following up cleavage with religation. Although the mutant proteins supported the essential function of Top2 in vivo, they conferred lethality in strains defective in the recombinational repair of DSBs or in the MRX complex. Consistent with elevated DSBs, overexpression of the Top2-FY,RG protein conferred hypersensitivity to Top2 poisons, was associated with a mitotic hyper-recombination phenotype, and led to elevated levels of covalent Top2-DNA complexes. This phenotype is consistent with the elevated DNA cleavage observed biochemically and is similar to that of etoposide in WT cells.

Although the Top2-FY,RG protein shows elevated cleavage, both amino acid substitutions map to the C-terminal dimer interface or "C-gate" region (Fig. 7*A*) rather than near the catalytic tyrosine. The C-gate constitutes the primary dimer interface that holds Top2 subunits together in the absence of DNA or ATP (47–49). During the Top2 catalytic cycle, this interface splits apart to allow a newly transported duplex that has crossed the cleaved-DNA segment to exit the enzyme (50). The stability of the C-gate interface, together with that of the nucleotide-dimerized ATPase domains, is thought to hold the two Top2 subunits together and guard against the accidental dissociation of the dimer during its duplex cleavage and passage reaction. Such dissociation would be expected to lead to persistent DSB formation.

A close-up of the interface shows that F1025 protrudes from the coiled-coil arms of the principal DNA-binding region and nestles into a small hydrophobic pocket on one side of the globular region of the C-gate (Fig. 7*B*). Given the location of F1025 and the protrusion of the tip of its benzyl ring so that it is solvent exposed, it seems unlikely that its replacement with tyrosine, which would project its phenolic oxygen into solution, would have an effect on C-gate stability. By comparison, R1128 packs against a tryptophan (W1122) that directly forms part of the dimer interface (Fig. 7*C*). This interaction, together with the introduction of a glycine in the middle of a helical element, would be expected to locally destabilize the region. Such destabilization could impact the integrity of the C-gate or the kinetics with which the dimer interface separates and reassociates. Either behavior could, in turn, detrimentally affect the cleavage propensity of Top2 and increase the lifetime of the cleaved DNA state, the possibility of subunit dissociation, or both.

The hyper-recombination phenotype associated with Top2-FY,RG expression in yeast, as well as the synthetic lethality in the absence of recombination, are consistent with stabilization of the cleavage intermediate. A mutator phenotype was not expected, however, which could reflect either the persistence of nicked intermediates (Fig. 2) or errors associated with the repair of DSBs. The sequencing of Can-R mutants was particularly informative, revealing a shift from predominantly base substitutions to a rarely observed type of insertion: de novo duplication of 2 to 4 bp of sequence. The largest class of duplications was 4 bp in size, which matches the distance between the nicks that Top2 makes on complementary DNA strands, and all duplications were NHEJ dependent. As illustrated on the left side of Fig. 8, the complete filling in of the 5′ overhangs generated by Top2 cleavage, followed by NHEJ-mediated ligation, creates a 4-bp duplication.

A composite spectrum of insertions >1 bp that were identified in the WT and *mre11-D56N* backgrounds (*SI Appendix*, Fig. S4) suggests the occurrence duplication hotspots. These could reflect sites of preferred Top2-FY,RG cleavage/stabilization or sites where end filling is more frequent and NHEJ is relatively error prone. The positions of Top2 cleavage can be inferred from 4-bp duplications, but not from smaller duplications. These cleavage

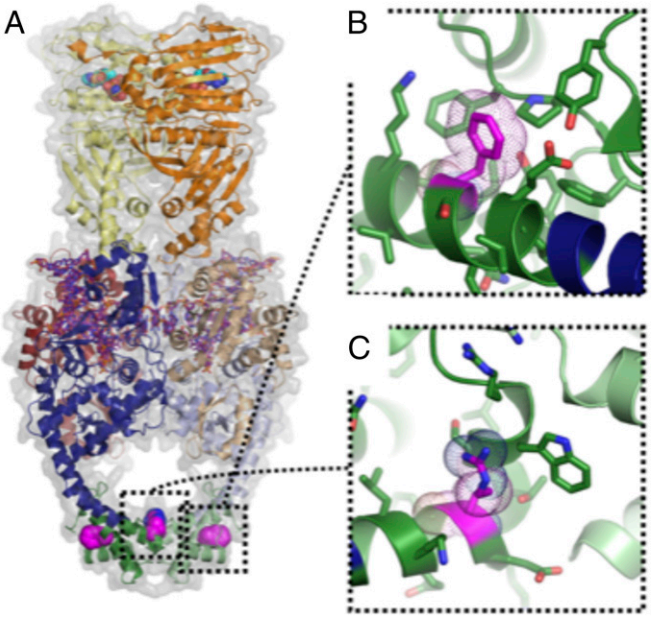

Fig. 7. The F1025Y/R1128G mutations map to the Top2 C-gate. (*A*) Cartoon representation of a full-length, nucleotide-bound *S. cerevisiae* Top2 dimer bound to a cleaved DNA segment (Protein Data Bank ID 4GFH) (46). One subunit is colored in dark hues and the other in light hues. Dark/light orange: ATPase domains; dark/light red: TOPRIM Mg2+-binding domain; dark/light blue: principal DNA-binding region; dark/light green: C-gate; dark purple: cleaved DNA. AMPPNP is shown as cyan spheres; the locations of F1025 and R1128 are marked as magenta spheres. (*B*) Close-up of the region around F1025 is highlighted, with F1025 shown in magenta. (*C*) Close-up of the region around R1128, illustrating the packing of this residue adjacent to W1122 at the dimer interface.

sites were aligned and analyzed for possible sequence conservation, such as the weak dyad symmetry reported for human TOP2 cleavage in vitro (51). Although none was observed in the nick-flanking region where the Top2 monomers are expected to contact DNA, there was a strong preference for AT base pairs in the region between the nicks (*SI Appendix*, Fig. S5). We suggest that the AT-richness may increase the stability of the cleavage intermediate or facilitate the strand separation that precedes the filling of 3′-recessed ends. Although stronger dyad symmetry has been associated with etoposide/VP16-stabilized human TOP2 and yeast Top2 cleavage intermediates (51, 52), there were not enough duplications identified following etoposide treatment to perform a similar analysis in the current study.

The Top2 cleavage site depicted in Fig. 8 corresponds to position 1007, where ~10% of the 4-bp duplications occurred (*SI Appendix*, Fig. S4). This position was also one of the few sites where 3-bp duplications were detected. The rarity of 3-bp duplications presumably reflects the fact that, unlike the 2- or 4-bp insertions, the addition of 3 bp maintains the correct reading frame of *CAN1* and rarely disables protein function. As illustrated in Fig. 8, 3-bp duplications can be readily formed at position 1007 by annealing the terminal nucleotide at each end of the TATT cleavage site and then filling the adjacent gaps. Three-base-pair duplications could also arise by removing a single nucleotide from one end of the DSB, followed by end filling and ligation. As illustrated in Fig. 8, 2-bp de novo duplications require the addition of 4 nt to one end and 2 nt to the other (or alternatively 3 nt to each end). If a Top2 cleavage site encompasses a dinucleotide repeat, however, misaligned pairing between complementary strands would seem the more likely mechanism. Finally, 1-bp insertions can be generated by partial filling of one or both ends or by misaligned pairing between the ends and subsequent gap filling. Based on the biochemistry of Top2, duplication sizes should not exceed the distance between the enzyme-generated nicks, and yet 21 of 163 (~13%) of the duplications were 5 bp. Eight of these occurred at a single position that increased a 5-bp repeat (GGGCT) from two copies to three and most likely reflected DNA polymerase slippage. The remainder were not in repetitive sequence and raise the intriguing possibility that Top2 monomers might occasionally create nicks that are 5 bp instead of 4 bp apart. Such altered spacing may be a specific feature associated with the *top2-FY,RG* allele or with other mutations that destabilize the dimer interface.

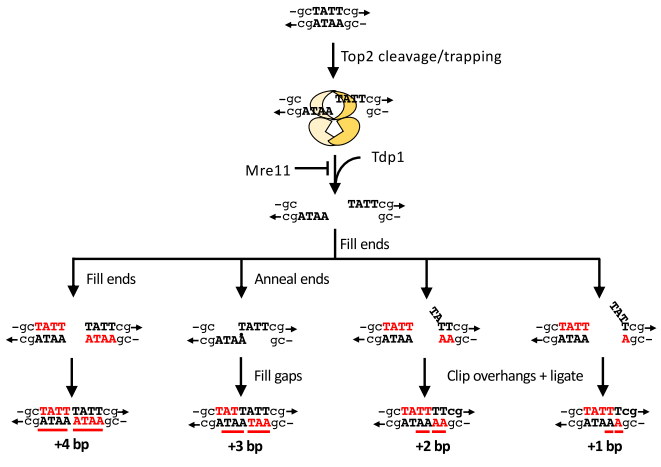

Fig. 8. Models for Top2-associated deletions. Complementary strands are shown with arrowheads indicating 3′ ends; the 4 bp flanked by Top2 nicks is in bold capital letters. Each Top2 monomer (different shades of yellow) uses an active-site tyrosine to nick one DNA strand, forming a covalent phosphotyrosyl bond with the 5′ end and creating a recessed 3′-OH end. Mre11 suppresses duplications by nicking the 5′-terminal strand and thereby removing Top2 as part of an oligonucleotide. Tdp1 cleaves the phosphotyrosyl bond to create a clean 5′ end. New bases added to recess 3′ ends after Top2 removal are in bold red font, and duplicated segments are underlined in red. There are multiple ways to generate 1- to 3-bp duplications that depend on where Top2 cleaves the duplex and if/how ends anneal before fill-in reactions.

Before end-filling and ligation can occur, the trapped Top2 must be removed from DNA ends. The increase in de novo duplications observed in the absence of Mre11 nuclease activity (*mre11-D56N* background) indicates that, as in higher eukaryotes (42), Top2 is primarily removed by the MRX-Sae2 complex (MRN-CtIP in mammals). In contrast to mammalian cells, however, the nuclease-dead Mre11 protein was compatible with viability; this difference may simply reflect a much lower load of persistent Top2 damage in the much smaller yeast genome or a more robust role of yeast Tdp1 in Top2cc removal from DNA ends. Although Mre11 nuclease activity was not required for viability in the presence of overexpressed Top2-FY,RG, it was necessary for the MRX complex to be present. This requirement does not reflect its essential role in yeast NHEJ, as NHEJ was dispensable for survival. In this context, the MRX complex may be required for mediating an appropriate checkpoint response (53).

In vitro, Mre11 nicks 15 to 40 nt from a 5′-blocked end (54), which precludes the end-filling required for de novo duplications. The 5′-end cleavage also facilitates more extensive end resection and commits repair to HR (55), although microhomology-mediated end joining is an alternative outcome if HR is not possible (56). It should be noted that the mutation assay done here was in haploid cells, where the only recombination option was the identical sister chromatid. The dramatic increase in de novo duplications in the absence of Mre11 nucleolytic activity indicates that MRX is the primary remover of trapped Top2, as it is in mammalian cells. Loss of Tdp1 had the reverse effect, and duplications were virtually eliminated. Although Tdp1 was originally identified as a phosphodiesterase that removes 3′-linked peptides from DNA (57), it also has been implicated in removal of 5′-linked peptides, and its loss confers etoposide sensitivity (41). It should be noted that yeast does not have a protein analogous to the TDP2 protein of mammals, which also is important for TOP2 removal (58) and suppresses chromosome rearrangements by creating DSB termini that are substrates for NHEJ (59).

The broader implications of the Top2-dependent mutation signature described here are two-fold and derive from the highly conserved biochemistry of Top2 and subsequent repair mechanisms. First, the stabilization of the covalent-cleavage intermediate by chemotherapeutic drugs, or the presence of an appropriate mutant TOP2 protein, is expected to have a similar consequence in mammalian cells. Insertions are much more likely to disrupt gene function than are base substitutions, with even a very low level having detrimental consequences. This may contribute to secondary malignancies that arise following the clinical use of TOP2 inhibitors, and the corresponding genomes would be expected to have a distinctive mutation signature. Mutations in TOP2 or protein overproduction could also be potential drivers of tumorigenesis. In this regard, we note that the yeast Top2 signature identified here matches insertion-deletion signature 17 (ID17) in human cancers, which is comprised primarily of 4-bp de novo duplications (60). A second implication of Top2-associated mutagenesis is that it provides a mechanism for the birth of repetitive sequences, as demonstrated here in yeast strains that overproduce the WT protein. In addition to its essential role during genome duplication, Top2 activity may thus be an important contributor to genome evolution.

Materials and Methods

Strains and Growth Conditions. A complete list of all yeast strains is provided in *SI Appendix*, Table S4. YPD medium was used for nonselective growth, and synthetic complete (SC) media missing one amino acid or base (e.g., SC-Ura

medium contained no uracil) were used for selective growth. For mitotic recombination experiments, diploid strains were grown in SC-Ura supplemented with peptone to improve growth. Can-R mutants were selected on SC-Arg plates containing 60 μg/mL L-canavanine sulfate. All growth was at 30 °C unless otherwise noted. Details of strain constructions, plasmid constructions, media, and growth conditions are in *SI Appendix*.

ICE Assay in Yeast. Log-phase *top2-4* cells containing a plasmid-encoded, HA-tagged *TOP2*, or *top2-FY,RG* allele were grown at 34 °C and treated with DMSO or DMSO + 20 μg/mL etoposide for 1 h. DNA-protein complexes were isolated using a cesium chloride gradient, treated with micrococcal nuclease, and separated using sodium dodecyl sulfate/polyacrylamide gel electrophoresis (SDS/PAGE). After transfer to a polyvinylidene fluoride membrane, Top2 covalent complexes were detected using an anti-HA (Santa Cruz, sc-805) or anti-Top2 (TopoGen, #TG2014) antibody. A detailed protocol can be found in *SI Appendix*.

Biochemical Assays. WT and mutant Top2 proteins were overexpressed in yeast and purified as previously described, as were relaxation assays (38). The same conditions were used for Top2 relaxation and cleavage reactions (38), but cleavage reactions were quenched with SDS instead of ethylenediaminetetraacetic acid. pUC18 was used as the DNA substrate and products were analyzed by agarose gel electrophoresis. Additional details are in *SI Appendix*.

Rate or Frequency Measurements and Mutation Analysis. Transformants containing the EV, pDED1Top2, or pDED1Top2-FY, RG plasmid were selected and subsequently maintained by growth in or on SC-Ura medium. Following growth of independent cultures to saturation, appropriate dilutions were plated to determine the number of viable cells or mutants/recombinants in each. For the etoposide experiments, cultures were grown to saturation in SC containing DMSO or DMSO + 200 μg/mL etoposide prior to plating. Rates or median frequencies were calculated as appropriate and 95% confidence intervals (CIs) were determined using table B11 in Altman et al. (61).

Independent Can-R or Lys^+ colonies were isolated using a pin-plating technique. Can-R mutants were sequenced in a high-throughput manner following the barcoding of each during PCR amplification. Pooled PCR products were sequenced using PacBio SMRT technology, and reads were sorted by barcodes for mutation identification. For analysis of Lys^+ revertants, the relevant portion of the *LYS2* gene was PCR amplified and analyzed by Sanger sequencing. The proportions of mutation types in different strains were compared using a contingency chi-square or Fisher exact test as appropriate (vassarstats.net); $P < 0.05$ was considered significant.

Mutation-type rates or frequencies were calculated by multiplying the total Can-R rate or frequency by the proportion of the mutation type in the corresponding spectrum. The corresponding 95% CI was determined by jointly considering the 95% CI for the Can-R rate or frequency and the 95% CI for the proportion (vassarstats.net) using the root of the square of the sums or right-triangle method (62). Rates or frequencies obtained in different strain backgrounds were considered significantly different if the respective 95% CIs did not overlap. Additional details are in *SI Appendix*.

Data Availability. All study data are included in the article and *SI Appendix*.

ACKNOWLEDGMENTS. We thank Steven Rozen (Duke-National University of Singapore Medical School) for pointing out that the yeast Top2 signature matches ID17 in the Catalog of Somatic Mutations in Cancer. Research was supported by NIH Grants R35 GM118077 (to S.J.-R.), R03 CA216010 (to J.L.N.), and R01 CA077373 (to J.B.).

1. J. B. Leppard, J. J. Champoux, Human DNA topoisomerase I: Relaxation, roles, and damage control. *Chromosoma* **114**, 75–85 (2005).
2. S. M. Vos, E. M. Tretter, B. H. Schmidt, J. M. Berger, All tangled up: How cells direct, manage and exploit topoisomerase function. *Nat. Rev. Mol. Cell Biol.* **12**, 827–841 (2011).
3. J. C. Wang, Moving one DNA double helix through another by a type II DNA topoisomerase: The story of a simple molecular machine. *Q. Rev. Biophys.* **31**, 107–144 (1998).
4. R. Ceccaldi, B. Rondinelli, A. D. D'Andrea, Repair pathway choices and consequences at the double-strand break. *Trends Cell Biol.* **26**, 52–64 (2016).
5. F. d'Adda di Fagagna, Living on a break: Cellular senescence as a DNA-damage response. *Nat. Rev. Cancer* **8**, 512–522 (2008).
6. W. P. Roos, B. Kaina, DNA damage-induced cell death: From specific DNA lesions to the DNA damage response and apoptosis. *Cancer Lett.* **332**, 237–248 (2013).
7. W. P. Roos, B. Kaina, DNA damage-induced cell death by apoptosis. *Trends Mol. Med.* **12**, 440–450 (2006).
8. J. L. Nitiss, Targeting DNA topoisomerase II in cancer chemotherapy. *Nat. Rev. Cancer* **9**, 338–350 (2009).
9. Y. Pommier, Drugging topoisomerases: Lessons and challenges. *ACS Chem. Biol.* **8**, 82–95 (2013).
10. J. L. Nitiss, DNA topoisomerase II and its growing repertoire of biological functions. *Nat. Rev. Cancer* **9**, 327–337 (2009).
11. N. G. Bush, K. Evans-Roberts, A. Maxwell, DNA topoisomerases. *Ecosal Plus* **6**, 26435256 (2015).
12. K. Evans-Roberts, A. Maxwell, DNA topoisomerases. *Ecosal Plus* **3**, 26443761 (2009).
13. J. L. Nitiss, K. C. Nitiss, A. Rose, J. L. Waltman, Overexpression of type I topoisomerases sensitizes yeast cells to DNA damage. *J. Biol. Chem.* **276**, 26708–26714 (2001).
14. P. Pourquier *et al*., Effects of uracil incorporation, DNA mismatches, and abasic sites on cleavage and religation activities of mammalian topoisomerase I. *J. Biol. Chem.* **272**, 7792–7796 (1997).
15. P. Pourquier *et al*., Induction of reversible complexes between eukaryotic DNA topoisomerase I and DNA-containing oxidative base damages. 7, 8-dihydro-8-oxoguanine and 5-hydroxycytosine. *J. Biol. Chem.* **274**, 8516–8523 (1999).
16. J. Sekiguchi, S. Shuman, Site-specific ribonuclease activity of eukaryotic DNA topoisomerase I. *Mol. Cell* **1**, 89–97 (1997).
17. N. Kim *et al*., Mutagenic processing of ribonucleotides in DNA by yeast topoisomerase I. *Science* **332**, 1561–1564 (2011).
18. J. L. Sparks, P. M. Burgers, Error-free and mutagenic processing of topoisomerase 1-provoked damage at genomic ribonucleotides. *EMBO J.* **34**, 1259–1269 (2015).
19. S. Y. Huang, S. Ghosh, Y. Pommier, Topoisomerase I alone is sufficient to produce short DNA deletions and can also reverse nicks at ribonucleotide sites. *J. Biol. Chem.* **290**, 14068–14076 (2015).
20. J. E. Cho *et al*., Parallel analysis of ribonucleotide-dependent deletions produced by yeast Top1 *in vitro* and *in vivo*. *Nucleic Acids Res.* **44**, 7714–7721 (2016).
21. K. C. Nitiss, J. L. Nitiss, L. A. Hanakahi, DNA damage by an essential enzyme: A delicate balance act on the tightrope. *DNA Repair (Amst.)* **82**, 102639 (2019).
22. P. S. Kingma, A. H. Corbett, P. C. Burcham, L. J. Marnett, N. Osheroff, Abasic sites stimulate double-stranded DNA cleavage mediated by topoisomerase II. DNA lesions as endogenous topoisomerase II poisons. *J. Biol. Chem.* **270**, 21441–21444 (1995).
23. Y. Wang, B. R. Knudsen, L. Bjergbaek, O. Westergaard, A. H. Andersen, Stimulated activity of human topoisomerases IIalpha and IIbeta on RNA-containing substrates. *J. Biol. Chem.* **274**, 22839–22846 (1999).
24. M. D. Megonigal, J. Fertala, M. A. Bjornsti, Alterations in the catalytic activity of yeast DNA topoisomerase I result in cell cycle arrest and cell death. *J. Biol. Chem.* **272**, 12801–12808 (1997).
25. N. A. Levin, M. A. Bjornsti, G. R. Fink, A novel mutation in DNA topoisomerase I of yeast causes DNA damage and RAD9-dependent cell cycle arrest. *Genetics* **133**, 799–814 (1993).
26. J. E. Cho, S. Jinks-Robertson, Topoisomerase I and genome stability: The good and the bad. *Methods Mol. Biol.* **1703**, 21–45 (2018).
27. J. V. Walker *et al*., A mutation in human topoisomerase II alpha whose expression is lethal in DNA repair-deficient yeast cells. *J. Biol. Chem.* **279**, 25947–25954 (2004).
28. K. Lehner, S. V. Mudrak, B. K. Minesinger, S. Jinks-Robertson, Frameshift mutagenesis: The roles of primer-template misalignment and the nonhomologous end-joining pathway in *Saccharomyces cerevisiae*. *Genetics* **190**, 501–510 (2012).
29. A. T. Rogojina, J. L. Nitiss, Isolation and characterization of mAMSA-hypersensitive mutants. Cytotoxicity of Top2 covalent complexes containing DNA single strand breaks. *J. Biol. Chem.* **283**, 29239–29250 (2008).
30. J. L. Nitiss *et al*., Amsacrine and etoposide hypersensitivity of yeast cells overexpressing DNA topoisomerase II. *Cancer Res.* **52**, 4467–4472 (1992).
31. C. Holm, T. Goto, J. C. Wang, D. Botstein, DNA topoisomerase II is required at the time of mitosis in yeast. *Cell* **41**, 553–563 (1985).
32. K. J. Dornfeld, D. M. Livingston, Effects of controlled *RAD52* expression on repair and recombination in *Saccharomyces cerevisiae*. *Mol. Cell. Biol.* **11**, 2013–2017 (1991).
33. J. Anand, Y. Sun, Y. Zhao, K. C. Nitiss, J. L. Nitiss, Detection of topoisomerase covalent complexes in eukaryotic cells. *Methods Mol. Biol.* **1703**, 283–299 (2018).
34. Y. Hsiung, S. H. Elsea, N. Osheroff, J. L. Nitiss, A mutation in yeast TOP2 homologous to a quinolone-resistant mutation in bacteria. Mutation of the amino acid homologous to Ser83 of *Escherichia coli gyrA* alters sensitivity to eukaryotic topoisomerase inhibitors. *J. Biol. Chem.* **270**, 20359–20364 (1995).
35. M. D. Rose, P. Novick, J. H. Thomas, D. Botstein, G. R. Fink, A Saccharomyces cerevisiae genomic plasmid bank based on a centromere-containing shuttle vector. *Gene* **60**, 237–243 (1987).
36. D. Subramanian, C. S. Furbee, M. T. Muller, ICE bioassay. Isolating in vivo complexes of enzyme to DNA. *Methods Mol. Biol.* **95**, 137–147 (2001).
37. G. N. Giaever, L. Snyder, J. C. Wang, DNA supercoiling *in vivo*. *Biophys. Chem.* **29**, 7–15 (1988).
38. J. L. Nitiss *et al*., Topoisomerase assays. *Curr. Protoc. Pharmacol.* **Chapter 3**, Unit 3.3 (2012).
39. M. Sander, T. Hsieh, Double strand DNA cleavage by type II DNA topoisomerase from *Drosophila melanogaster*. *J. Biol. Chem.* **258**, 8421–8428 (1983).
40. J. M. Daley, P. L. Palmbos, D. Wu, T. E. Wilson, Nonhomologous end joining in yeast. *Annu. Rev. Genet.* **39**, 431–451 (2005).
41. K. C. Nitiss, M. Malik, X. He, S. W. White, J. L. Nitiss, Tyrosyl-DNA phosphodiesterase (Tdp1) participates in the repair of Top2-mediated DNA damage. *Proc. Natl. Acad. Sci. U.S.A.* **103**, 8953–8958 (2006).
42. N. N. Hoa *et al*., Mre11 is essential for the removal of lethal topoisomerase 2 covalent cleavage complexes. *Mol. Cell* **64**, 580–592 (2016).

43. E. L. Baldwin, A. C. Berger, A. H. Corbett, N. Osheroff, Mms22p protects *Saccharomyces cerevisiae* from DNA damage induced by topoisomerase II. *Nucleic Acids Res.* **33**, 1021–1030 (2005).
44. S. Moreau, J. R. Ferguson, L. S. Symington, The nuclease activity of Mre11 is required for meiosis but not for mating type switching, end joining, or telomere maintenance. *Mol. Cell. Biol.* **19**, 556–566 (1999).
45. M. Jannatipour, Y. X. Liu, J. L. Nitiss, The *top2-5* mutant of yeast topoisomerase II encodes an enzyme resistant to etoposide and amsacrine. *J. Biol. Chem.* **268**, 18586–18592 (1993).
46. B. H. Schmidt, N. Osheroff, J. M. Berger, Structure of a topoisomerase II-DNA-nucleotide complex reveals a new control mechanism for ATPase activity. *Nat. Struct. Mol. Biol.* **19**, 1147–1154 (2012).
47. J. Roca, J. C. Wang, The capture of a DNA double helix by an ATP-dependent protein clamp: A key step in DNA transport by type II DNA topoisomerases. *Cell* **71**, 833–840 (1992).
48. J. Roca, J. C. Wang, DNA transport by a type II DNA topoisomerase: Evidence in favor of a two-gate mechanism. *Cell* **77**, 609–616 (1994).
49. J. M. Berger, S. J. Gamblin, S. C. Harrison, J. C. Wang, Structure and mechanism of DNA topoisomerase II. *Nature* **379**, 225–232 (1996).
50. J. Roca, J. M. Berger, S. C. Harrison, J. C. Wang, DNA transport by a type II topoisomerase: Direct evidence for a two-gate mechanism. *Proc. Natl. Acad. Sci. U.S.A.* **93**, 4057–4062 (1996).
51. G. Capranico, K. W. Kohn, Y. Pommier, Local sequence requirements for DNA cleavage by mammalian topoisomerase II in the presence of doxorubicin. *Nucleic Acids Res.* **18**, 6611–6619 (1990).
52. W. H. Gittens *et al*., A nucleotide resolution map of Top2-linked DNA breaks in the yeast and human genome. *Nat. Commun.* **10**, 4846 (2019).
53. T. T. Paull, 20 Years of Mre11 biology: No end in sight. *Mol. Cell* **71**, 419–427 (2018).
54. E. Cannavo, G. Reginato, P. Cejka, Stepwise 5′ DNA end-specific resection of DNA breaks by the Mre11-Rad50-Xrs2 and Sae2 nuclease ensemble. *Proc. Natl. Acad. Sci. U.S.A.* **116**, 5505–5513 (2019).
55. L. S. Symington, J. Gautier, Double-strand break end resection and repair pathway choice. *Annu. Rev. Genet.* **45**, 247–271 (2011).
56. A. Sfeir, L. S. Symington, Microhomology-mediated end joining: A back-up survival mechanism or dedicated pathway? *Trends Biochem. Sci.* **40**, 701–714 (2015).
57. J. J. Pouliot, K. C. Yao, C. A. Robertson, H. A. Nash, Yeast gene for a Tyr-DNA phosphodiesterase that repairs topoisomerase I complexes. *Science* **286**, 552–555 (1999).
58. Y. Pommier *et al*., Tyrosyl-DNA-phosphodiesterases (TDP1 and TDP2). *DNA Repair (Amst.)* **19**, 114–129 (2014).
59. F. Gómez-Herreros *et al*., TDP2 suppresses chromosomal translocations induced by DNA topoisomerase II during gene transcription. *Nat. Commun.* **8**, 233 (2017).
60. L. B. Alexandrov *et al*.; PCAWG Mutational Signatures Working Group; PCAWG Consortium, The repertoire of mutational signatures in human cancer. *Nature* **578**, 94–101 (2020).
61. D. G. Altman, *Practical Statistics for Medical Research*, (CRC Press, New York, ed. 1, 1990), p. 611.
62. A. Moore *et al*., Genetic control of genomic alterations induced in yeast by interstitial telomeric sequences. *Genetics* **209**, 425–438 (2018).